

## Effect of Conductive Additives on the Structural and Electrochemical Properties of $\text{Li}_4\text{Ti}_5\text{O}_{12}$ Spinel

Jae-Hwan Park, Seongsu Lee,<sup>†,\*</sup> Sung-Soo Kim,<sup>\*</sup> and Jong-Huy Kim<sup>‡</sup>

Graduate School of Green Energy Technology, Chungnam National University, Daejeon 305-764, Korea

<sup>\*</sup>E-mail: kimss@cnu.ac.kr

<sup>†</sup>Neutron Science Division, Korea Atomic Energy Research Institute, Daejeon 305-353, Korea. <sup>\*</sup>E-mail: seongsulee@kaeri.re.kr

<sup>‡</sup>Korea Institute of Energy Research, Daejeon 305-343, Korea

Received August 31, 2012, Accepted September 17, 2012

The effect of a conductive agent on the structural and electrochemical properties of  $\text{Li}_4\text{Ti}_5\text{O}_{12}$  (LTO) spinel was investigated through neutron diffraction during Li intercalation and electrochemical measurements. The charging process of LTO is known as transformation of the white  $(\text{Li}_3)_{8a}[\text{LiTi}_5]_{16d}\text{O}_{12}$  into a dark-colored  $(\text{Li}_{3-x})_{8a}[\text{Li}_{x+y}]_{16c}[\text{LiTi}_5]_{16d}\text{O}_{12}$  by incorporating the inserted Li into octahedral 16c sites, and the Li in tetrahedral 8a sites shifted to 16c sites. The occupancy of the tetrahedral 8a site varied with the existence of carbon in the electrode. Without carbon, the lattice parameter and cell volume of LTO decreased more notably than in the carbon-containing LTO electrode during Li insertion process. These phenomena might be attributed that the Li occupancy of the tetrahedral 8a of the LTO electrode without carbon was less than that of the carbon-containing LTO electrode.

**Key Words :** Lithium ion batteries, Lithium titanate, Carbon additive effect, Neutron diffraction

### Introduction

Rechargeable lithium-ion batteries are becoming increasingly important as power sources for portable electronic devices, and their large-scale application to vehicles is being intensively pursued. Their major challenges, however, in terms of safety, quick charging, and life cycle, inhibit their further use in price-sensitive and large-scale applications.

Recently, the  $\text{Li}_4\text{Ti}_5\text{O}_{12}$  spinel has been focused on as an anode in large-scale batteries due to its safety, high-rate capability, and long life.<sup>1-3</sup> It is well known that lithium insertion into  $\text{Li}_4\text{Ti}_5\text{O}_{12}$  is accompanied by very slight changes in the lattice dimensions, although several experiment results differ as to whether the lattice expands or shrinks with the insertion of Li ions.<sup>4,5</sup>  $\text{Li}_4\text{Ti}_5\text{O}_{12}$ , however, as a zero strain material, is considered ideal for long-life rechargeable batteries.

The other key feature of  $\text{Li}_4\text{Ti}_5\text{O}_{12}$  is that it has the unusual combination of an excellent rate capability and an extremely flat plateau (-1.55 V), unlike Li metal, due to the two-phase reaction between  $\text{Li}_4\text{Ti}_5\text{O}_{12}$  and  $\text{Li}_7\text{Ti}_5\text{O}_{12}$ .<sup>5</sup> In  $\text{Li}_4\text{Ti}_5\text{O}_{12}$ , all tetrahedral 8a sites are occupied by Li, which results in  $(\text{Li}_3)_{8a}[\text{LiTi}_5]_{16d}(\text{O}_{12})_{32e}$ . The low electrical conductivity of the  $\text{Li}_4\text{Ti}_5\text{O}_{12}$  spinel suggests that the 8a tetrahedral positions are occupied.<sup>6</sup> Lithiation leads to 16c occupation and induces Li ions to move from 8a to 16c positions, most likely because of the coulomb repulsion between the nearest Li ions that occupy the 8a-16c positions and that are separated only by 1.81 Å. Finally, all the electrochemically active Li ions occupy the octahedral 16c site, which results in the anticipated end composition  $[\text{Li}_6]_{16c}[\text{LiTi}_5]_{16d}(\text{O}_{12})_{32e}$ . In terms of electronic conductivity, a large difference between  $\text{Li}_4\text{Ti}_5\text{O}_{12}$  and lithiated  $\text{Li}_7\text{Ti}_5\text{O}_{12}$  can be realized, although

these end members show subtle changes in their lattice dimensions.

The electrode material for Li ion batteries requires good conductivity – *i.e.*, both electronic and  $\text{Li}^+$  ionic conductivity. Many researchers recently reported the remarkable improvement of the electronic conductivity of  $\text{Li}_4\text{Ti}_5\text{O}_{12}$  through Mg doping<sup>7</sup> and size control.<sup>8</sup> In the case of size control, the occupancy of the tetrahedral 8a site increased as the particle size decreased.<sup>8</sup> The most common and practical method of enhancing the conductivity of an electrode is adding a conductive agent to the electrode without causing capacity loss of its active materials. The question arises, whether or not there is still a need for conductive agents for the lithiated  $\text{Li}_7\text{Ti}_5\text{O}_{12}$  that has fully or partially occupied the Li octahedral 16c. If there is no more need for conductive agent, the influence of the structure without conductive agents on the electrochemical properties must be known.

This research was conducted to study in detail the  $\text{Li}_{4+x}\text{Ti}_5\text{O}_{12}$  structure with the conductive agent carbon and to give better understanding the relation of crystal structure of mixed 8a/16c occupation with electrochemical properties during Li insertion.

### Experiment

In this study, the white crystalline  $\text{Li}_4\text{Ti}_5\text{O}_{12}$  powders provided by Samsung Fine Chemicals were used. Their morphology was observed with a field emission scanning microscope (FE-SEM: JSM-6300).

The two kinds of LTO electrodes (samples M and Y) were fabricated from a mixture of active materials, conductive agents DB (Denka Black), and polyvinylidene fluoride (PVDF)

at a weight ratio of 80:10:10 (sample Y) and 90:0:10 (sample M). *N*-Methyl pyrrolidone (NMP) was used to make slurry of the mixture. After the slurry was homogenized with a mixer (Thinky mixer-ARE310) at a high speed (2,000 rpm) for 20 minutes, it was coated with an aluminum foil and dried at 100 °C for 12 h. Then the electrode was roll-pressed and the disks were punched out.

The electrochemical performance of the two kinds of LTO electrodes was evaluated with CR2032-type coin cells. Lithium metal foil was used as the counter electrode, and the Celgard 2500 commercialized film, as the separator. The cells were assembled in a dry box with an inert argon atmosphere. The electrolyte solution was 1 M  $\text{LiPF}_6$  in a mixture of ethylene carbonate (EC), dimethyl carbonate (DMC), and ethylmethyl carbonate (EMC) (at a 1:1:1 volume ratio). The electrochemical properties were examined at a current density of 0.1 C (15 mA/g) between 1–3 V at room temperature, and the impedance was measured at each state-of-charge (SOC) level with Ivium n-Stat. At each SOC level, the cells were disassembled and the electrodes were rinsed in a DMC solvent several times in the dry box with an inert Ar atmosphere to remove the Li salt from the surface, and then dried for more than 2 h, after which the Al foil of the current collector was removed and powder samples of M and Y at each SOC level were prepared to measure the neutron diffraction.

The neutron diffraction data were collected over a  $2\theta$  range of 0–160° with a step size of 0.05°, and  $\lambda = 1.8348 \text{ \AA}$  was supplied by a Ge (331) single-crystal monochromator on a high-resolution powder diffractometer (HRPD) at HANARO at the Korea Atomic Energy Research Institute. The resulting neutron diffraction spectra were refined using the Rietveld method with the Fullproof program.<sup>9</sup>

## Results and Discussion

Figure 1 shows the powder morphology of the white LTO sample. It shows 300 to 400 nm primary particles agglomerated spherically to 7 to 8 micron secondary particles. A larger surface area could be assumed for the Li reaction than that for the monolithic powder through the existence of the internal pore in the secondary particles of the LTO sample. The XRD measurement showed that the used LTO powders had a cubic space group of  $Fd\bar{3}m$  without obvious impurities. Figure 2(a) shows the charge/discharge voltage profiles of the LTO samples of Y-LTO and M-LTO with and without conductive agents DB (Denka Black), respectively. Both samples of the Y and M electrodes showed more than 2.8 mol of Li inserted into the  $\text{Li}_4\text{Ti}_5\text{O}_{12}$ , which is more than 90% of the theoretical amount, down to 1 V, versus in  $\text{Li}/\text{Li}^+$ . In the electrochemical cycle, the results of the Y sample showed a larger capacity and low overpotential voltage profiles than those of the M sample. It is natural to assume that the conductive agents enhanced the electronic conductivity of the electrode, and thus, a small resistance yields a slightly larger capacity and a low overpotential. The extremely flat voltage of around 1.55 V was observed in both the M and Y

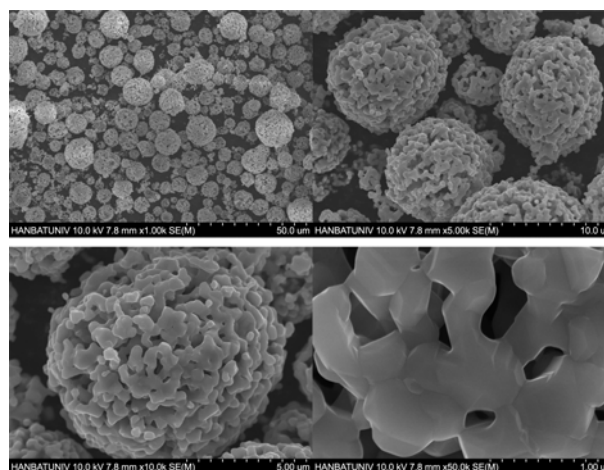


**Figure 1.** SEM images of white  $\text{Li}_4\text{Ti}_5\text{O}_{12}$  powder sample. Magnified agglomerated particles show the pore contained features.

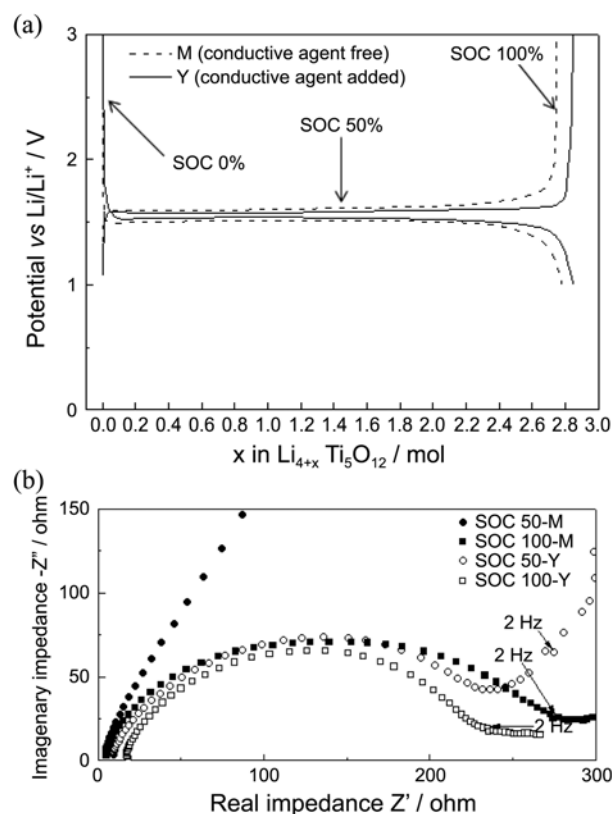


**Figure 2.** (a) Discharge and charge voltage profile. (b) Impedance plot of sample M and Y half cell at each SOC levels.

samples, which suggests a two-phase reaction,<sup>4,5</sup> although the fast (dis)charging property requires a single-phase reaction rather than a two-phase reaction. Figure 2(b) shows the impedance spectrum of the M and Y electrodes at the SOC levels of 50% and 100%. It was no surprise that there was no remarkable difference between the 100% SOC impedances of the M and Y samples, whereas there was a wide gap between the 50% SOC impedances of the M and Y samples. Due to the insulating nature of  $\text{Li}_4\text{Ti}_5\text{O}_{12}$ , it can be assumed that the 50% SOC impedance of sample M is much larger

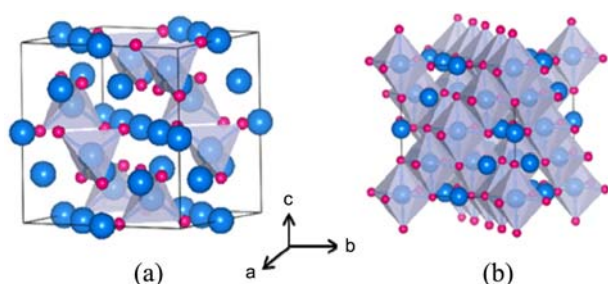


**Figure 3.** Crystal structures of (a) white insulator  $\text{Li}_4\text{Ti}_5\text{O}_{12}$  and (b) dark-colored conductor  $\text{Li}_7\text{Ti}_5\text{O}_{12}$ .

than that of sample Y. Moreover, in the case of the 100% SOC, the charged  $\text{Li}_7\text{Ti}_5\text{O}_{12}$  became metallic after the inserted Li ions occupied the octahedral 16c and after the partial transfer of Li ions from the tetrahedral 8a to 16c.<sup>10</sup> Figure 3 shows the crystal structure of  $\text{Li}_4\text{Ti}_5\text{O}_{12}$  and  $\text{Li}_7\text{Ti}_5\text{O}_{12}$ , which is known as space group  $\text{Fd-}3\text{m}$ . The discrete tetrahedral (8a) sites are occupied by Li in  $\text{Li}_4\text{Ti}_5\text{O}_{12}$  (Fig. 3(a)), whereas edge shared octahedral site (16c) are occupied in (Fig. 3(b)). It is well known that this structure differences are closely linked to the sample color and electrical conductivity.<sup>3,12</sup>

One of the most unique features of LTO is its zero strain properties with Li insertion. This means that with lithium insertion or removal, the lattice constant changes between  $\text{Li}_4\text{Ti}_5\text{O}_{12}$  and  $\text{Li}_7\text{Ti}_5\text{O}_{12}$  become almost zero.<sup>4</sup> The structural changes were not confirmed *via* XRD. Since the scattering factor of the  $\text{Li}^+$  ions is small compared to that of the  $\text{Ti}^{4+}$  and  $\text{O}^{2-}$  ions, it might be assumed that there were only small changes in the X-ray diffraction during the reaction with Li. Therefore, neutron diffraction was performed to analyze the structure, such as the lattice parameter and Li occupancy variation, with the conductive agents during the lithiation.

The structural variation was refined through neutron diffraction. The lattice parameter variation with SOC is shown in Figure 4. Table 1 shows the refinement details. The lattice parameter decreased with Li insertion in both the M and Y samples. The reduction of the lattice parameter with Li insertion has been reported before with experimental values and calculations.<sup>5,8,12</sup> This lattice shrink has been explained

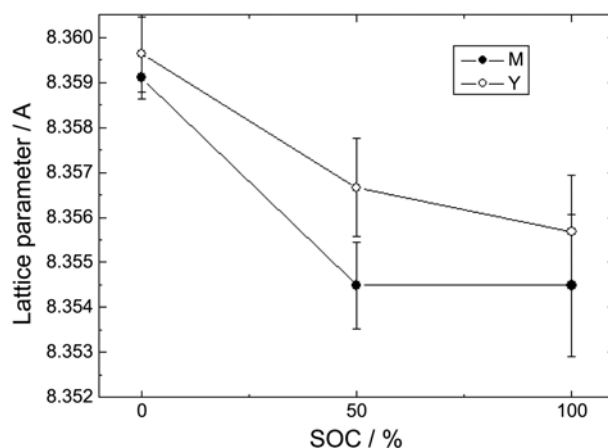


**Figure 4.** Lattice parameter variation with SOC of sample M and Y.

as the change in the Li positions from the 8a site to the 16c site.<sup>5,12</sup> In the samples in this study, it was clear that the existence of conductive agents influenced the reduction of the lattice parameter with Li insertion. Before the lithiation, the lattice parameters of samples M and Y are almost the same values, but the lattice parameter of sample M decreased further comparing sample Y at the 50% SOC level. This might be thought that the conductive agents surrounding LTO release the coulombic repulsion at the particle surface during initial lithiation process. The occupancy of the Li ions of the 8a and 16c sites was refined from lattice parameter through the neutron diffraction results. All the agreement factor of these refinements was reliable value as shown in Table 1. In sample Y, the transfer amounts of the Li ions from 8a to 16c were less than that of sample M, which was linked to smaller lattice parameter decrease in sample Y than that in sample M. Similar phenomena with respect to the partial occupancy variation of 8a and 16c with the particle size have been reported.<sup>8,11</sup> The results with micrometer-sized samples showed full occupancy of the octahedral 16c site, whereas partial occupancy of the tetrahedral 8a site in nano-sized samples. It is interesting that the existence of conductive agents in the electrode affected the Li occupancy of the 8a and 16c sites during charging. As shown in Figure

**Table 1.** Neutron diffraction refinement results with SOC of sample M and Y

SOC (%)	M sample				Y sample			
	Occupancy of Li		Lattice parameter (Å)	Agreement factor (%)	Occupancy of Li		Lattice parameter (Å)	Agreement factor (%)
	8a	16c			8a	16c		
0	3.00	0	8.3591	$R_p = 2.85$ $R_{wp} = 3.67$ $R_{exp} = 1.95$	3.00	0	8.3596	$R_p = 3.41$ $R_{wp} = 4.34$ $R_{exp} = 2.05$
50	2.556	1.944	8.3545	$R_p = 2.92$ $R_{wp} = 3.75$ $R_{exp} = 2.20$	3.00	1.50	8.3567	$R_p = 3.27$ $R_{wp} = 4.15$ $R_{exp} = 2.05$
100	2.222	3.779	8.3545	$R_p = 3.33$ $R_{wp} = 4.27$ $R_{exp} = 2.24$	2.884	3.118	8.3557	$R_p = 2.95$ $R_{wp} = 3.73$ $R_{exp} = 2.10$

2, the electrochemical properties were not influenced with the different Li occupancy rates of 8a and 16c. Although the voltage profile of sample Y showed less hysteresis than that of sample M, there were almost the same impedance values in the fully charged samples. These electrochemical properties and the structure variation results of sample M and Y can suggest that the mixed 8a/16c occupation had a beneficial effect in aspect of high ionic mobility and high power performance of the LTO-based electrodes.

### Conclusions

It was seen that the occupation ratio of the 16c/8a site, during the lithiation of  $\text{Li}_{4+X}\text{Ti}_5\text{O}_{12}$  to up to  $X = 3$ , varied with the conductive agent included in the electrodes through the neutron diffraction refinements. These results differed from those of the previous study, in which the Li ions at the 8a site shifted to the 16c site, and improved the electrical conductivity that composed the linked  $\text{LiO}_6$  octahedra. There was no remarkable gap between the 100% SOC samples of the conductive-agent-free and -included electrodes. This implies that the conductivity was enhanced by the mixed 8a/16c occupation and the related defect existence, and not only by the shift in the Li ions to the 16c site. In addition to the zero strain properties of the LTO material, which are regarded as the main factors of long-cycle-life durability, the mixed occupation of the 8a/16c site had the most remarkable characteristics that were responsible for the high ionic mobility.

**Acknowledgments.** This work was financially supported by Korea Institute of Energy Research (KIER) and the Nuclear Research and Development Program of the Korea Science and Engineering Foundation. This work was also supported by the Chungnam National University, Korea.

### References

1. Kavan, L.; Prochazka, J.; Spitzler, T. M.; Kalbac, M.; Jukalova, M.; Drezen, T.; Gratzel, M. *J. Electrochem. Soc.* **2003**, *150*, A1000.
2. Belharouak, I.; Sun, Y.-K.; Lu, W.; Lin, J.; Amine, K. *J. Electrochem. Soc.* **2007**, *154*, A1083.
3. Takami, N.; Inagaki, H.; Kishi, T.; Harada, Y.; Fujita, Y.; Hoshina, K. *J. Electrochem. Soc.* **2009**, *156*, A128.
4. Ohzuku, T.; Ueda, A.; Yamamoto, N. *J. Electrochem. Soc.* **1995**, *142*, 1431.
5. Scharner, S.; Weppner, W.; Beaurmann, P. S. *J. Electrochem. Soc.* **1999**, *146*, 857.
6. Leonidov, I. A.; Leonidova, O. N.; Perelyaeva, L. A.; Samigullina, R. F.; Kovyazina, S. A.; Patrakeeve, M. V. *Phys. Solid State* **2003**, *45*, 2183.
7. Chen, C. H.; Vaughey, J. T.; Jansen, A. N.; Dees, D. W.; Kahaian, A. J.; Goacher, T.; Thackeray, M. M. *J. Electrochem. Soc.* **2001**, *148*, 103.
8. Borghols, W. J. H.; Wagemaker, M.; Lafont, U.; Kelder, E. M.; Mulder, F. M. *J. Am. Chem. Soc.* **2009**, *131*, 17786.
9. Rodríguez-Carvajal, J. *Physica B* **1993**, *55*, 192.
10. Wagemaker, M.; Simon, D. R.; Kelder, E. M.; Schoonman, J.; Ringpfeil, C.; Haake, U.; Hecht, D. L.; Frahm, R.; Mulder, F. M. *Adv. Mater.* **2006**, *18*, 3169.
11. Wagemaker, M.; van Eck, E. R. H.; Kentgens, A. P. M.; Mulder, F. M. *J. Phys. Chem. B* **2009**, *113*, 224.
12. Ouyang, C. Y.; Zhong, Z. Y.; Lei, M. S. *Electrochem. Commun.* **2007**, *9*, 1107.